Journal of Medicinal Chemistry Article

J. Med. Chem. **2010,** *53,* 4603–4614 **4603**
DOI: 10.1021/jm100210p

Selective GlyT1 Inhibitors: Discovery of [4-(3-Fluoro-5-trifluoromethylpyridin-2-yl)piperazin-1-yl]-[5-methanesulfonyl-2-((*S*)-2,2,2-trifluoro-1-methylethoxy)phenyl]methanone (RG1678), a Promising Novel Medicine To Treat Schizophrenia

Emmanuel Pinard,* Alexander Alanine, Daniela Alberati, Markus Bender, Edilio Borroni, Patrick Bourdeaux, Virginie Brom, Serge Burner, Holger Fischer, Dominik Hainzl, Remy Halm, Nicole Hauser, Synese Jolidon, Judith Lengyel, Hans-Peter Marty, Thierry Meyer, Jean-Luc Moreau, Roland Mory, Robert Narquizian, Mathias Nettekoven, Roger D. Norcross, Bernd Puellmann, Philipp Schmid, Sebastien Schmitt, Henri Stalder, Roger Wermuth, Joseph G. Wettstein, and Daniel Zimmerli

F. Hoffmann-La Roche Ltd., Pharmaceutical Division, CH-4070 Basel, Switzerland

Received February 17, 2010

The GlyT1 transporter has emerged as a key novel target for the treatment of schizophrenia. Herein, we report on the optimization of the 2-alkoxy-5-methylsulfonebenzoylpiperazine class of GlyT1 inhibitors to improve hERG channel selectivity and brain penetration. This effort culminated in the discovery of compound **10a** (RG1678), the first potent and selective GlyT1 inhibitor to have a beneficial effect in schizophrenic patients in a phase II clinical trial.

Introduction

Schizophrenia is a severe and chronic mental illness with prevalence estimates ranging from 0.5% to 1% of the population. Symptoms of schizophrenia, which typically emerge during adolescence or early adulthood, are broadly categorized as positive, negative, or cognitive. The leading treatments for this central nervous system (CNS[a]) disorder are the atypical antipsychotics belonging to the family of dopamine D2 and serotonin 5-HT2a receptor antagonists. These drugs are efficacious in the management of positive symptoms; however, they demonstrate minimal effects on negative symptoms and cognitive function. In addition, because of their promiscuous pharmacology, these medicines have unsatisfactory side effect profiles. There is therefore a clear need to develop novel nondopaminergic/nonserotonergic approaches that may enable the identification of more efficacious and safer therapeutic agents.[1] Over the past 2 decades, preclinical and clinical evidence has accumulated suggesting that hypofunction of glutamatergic *N*-methyl-D-aspartate (NMDA) receptors may play an important role in the pathophysiology of schizophrenia.[2] Thus, therapeutic intervention aiming at restoring NMDA receptor activity may represent a promising novel avenue for the management of this disorder. As glycine is an obligatory coagonist at the NMDA receptor complex,[3] one approach to enhance NMDA receptor activity is to elevate extracellular levels of glycine in the brain through selective inhibition of glycine uptake mediated by the glycine transporter-1 (GlyT1) which is coexpressed with the NMDA receptor.[4] Strong support for this approach comes from clinical studies where glycine and D-serine, which are both coagonists at the glycine site of the NMDA receptor and sarcosine, a prototypical weak GlyT1 inhibitor, improved positive, negative, and cognitive symptoms in schizophrenic patients when added to conventional therapy.[5] As sarcosine has a poor pharmacokinetic profile and therefore is not an optimal therapeutic agent, considerable effort has been focused on the development of improved selective GlyT1 inhibitors.[6] The first reported set of examples were designed by chemical modification of sarcosine and included compounds **1**,[7] **2**,[8] and **3** (Figure 1).[9] However, it was soon realized that many sarcosine derivatives suffered from a range of undesirable effects including hypoactivity, ataxia, and reduced respiratory activity.[10,11] Consequently, these findings led a large number of pharmaceutical companies to orient their GlyT1 medicinal chemistry programs toward the identification of non-sarcosine-based inhibitors. This broad drug discovery effort successfully delivered a rich set of highly structurally diverse non-amino-acid chemotypes as exemplified by the selected compounds **4**,[12] **5**,[13] and **6**[14] (Figure 1). We have also contributed to this field and described the optimization of the non-sarcosine-based spiropiperidine **7**.[15]

More recently, we reported on the discovery of benzoylpiperazines as a further novel chemotype of GlyT1 inhibitors.[16] Starting from high-throughput screening (HTS) hit **8** (GlyT1 EC_{50} = 15 nM), SAR studies accompanied by the early assessment of molecular properties and metabolic stability of the synthesized derivatives led to the identification of a

*To whom correspondence should be addressed. Phone: +41 61 688 43 88. Fax: +41 61 688 87 14. E-mail: emmanuel.pinard@roche.com.

[a] Abbreviations: Boc, *tert*-butyloxycarbonyl; CNS, central nervous system; CYP450, cytochrome P450; DMF, *N*,*N*-dimethylformamide; DMPK, drug metabolism and pharmacokinetic; EWG: electron withdrawing group; FaSSIF, fasted state simulated intestinal fluid; FeSSIF, fed state simulated intestinal fluid; GlyT1, glycine transporter 1; hERG, human ether-a-go-go-related gene; HPLC, high pressure liquid chromatography; HTS, high-throughput screening; iv, intravenous; MNT, micronucleus test; NMDA, *N*-methyl-D-aspartate; NMP, *N*-methylpyrrolidone; po, per os (oral); PAMPA, parallel artificial membrane permeation assay; PPB, plasma protein binding; SAR, structure−activity relationship; TBTU, 2-(1*H*-benzotriazole-1-yl)-1,1,3,3-tetramethyluronium tetrafluoroborate; THF, tetrahydrofuran; THP, tetrahydropyranyl; TLC, thin layer chromatography; TPGS, D-α-tocopheryl polyethylene glycol 1000 succinate.

Published on Web 05/21/2010

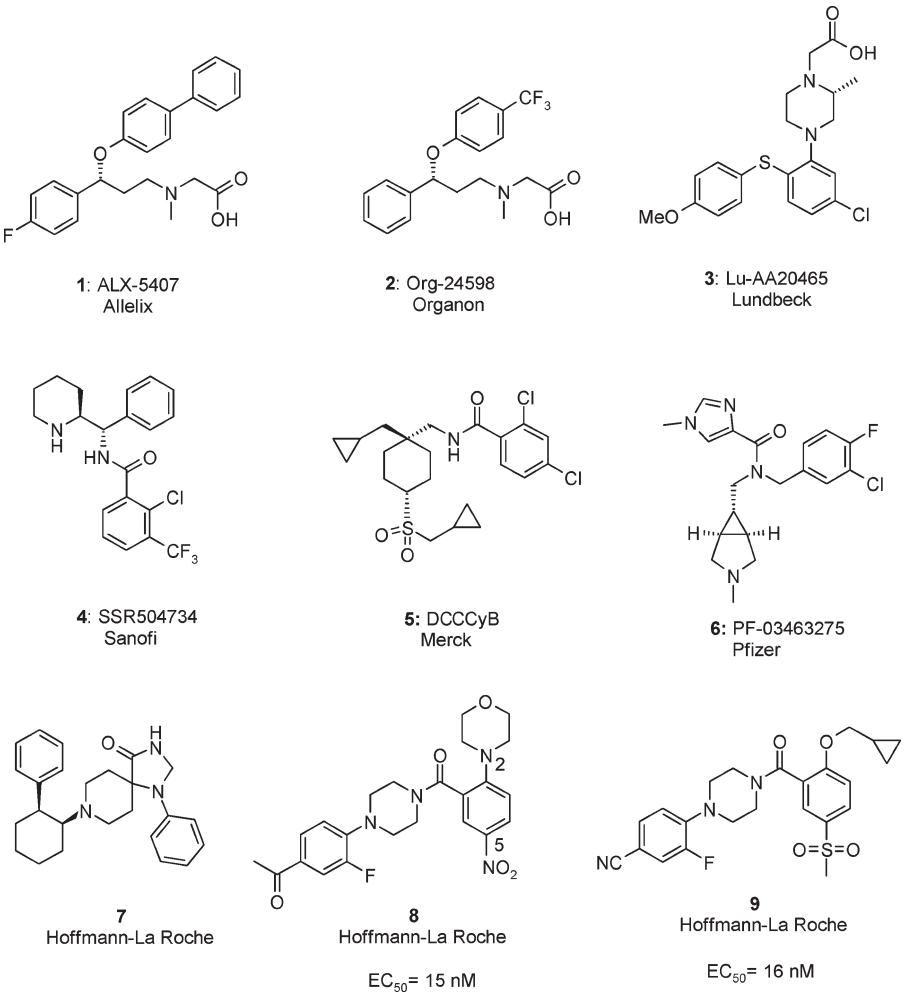

Figure 1. A selection of published GlyT1 inhibitors.

highly promising subseries in which the morpholine and nitro residues in positions 2 and 5 in **8** (Figure 1) were replaced respectively by an alkoxy and a methyl sulfone group. Within this 2-alkoxy-5-methylsulfonebenzoylpiperazine subseries, highly potent, selective, and druglike GlyT1 inhibitors were identified, demonstrating in particular excellent metabolic stabilities, oral bioavailabilities, and no significant inhibition of the major metabolizing CYP450 enzymes. Moreover, in an in vivo microdialysis study in which the extracellular fluid in the striatum of mice was sampled by means of an implanted microdialysis probe, representative compound **9** (GlyT1 EC_{50} = 16 nM) induced a robust and sustained increase level of glycine after oral administration, providing evidence that **9** acts in vivo as a GlyT1 inhibitor. Furthermore, we have found that our benzoylpiperazines were able to dose-dependently reverse the hyperlocomotion induced in mice by (3*R*,4*R*)-3-amino-1-hydroxy-4-methylpyrrolidin-2-one (L-687,414),[17] a known selective and brain-penetrating glycine site NMDA receptor antagonist. An ID_{50} (dose producing 50% inhibition of L-687,414-induced hyperlocomotion) of 3 mg/kg was measured for compound **9** after oral administration (Figure 2). Such behavioral effect was observed as well with the potent and brain penetrant published GlyT1 inhibitors we have tested. For example, with sarcosine-based compound **2**, an ID_{50} of 0.6 mg/kg po was measured.[18] In contrast, no effect was seen with the selective GlyT2 inhibitor 4-benzyloxy-*N*-(1-dimethylaminocyclopentylmethyl)-3,5-dimethoxybenzamide

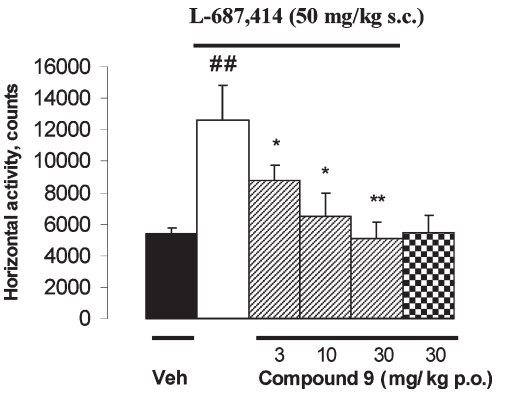

Figure 2. Dose-dependent inhibition of L-687,414-induced hyperlocomotion by compound **9** in mice. The data represent mean horizontal activity counts per group recorded over a 60 min time period. Error bars indicate SEM (n = 8 per group): (##) $p < 0.01$ versus vehicle (Veh) alone; (*) $p < 0.05$, (**) $p < 0.01$ versus L-687,414 alone.

(Org-25543),[19] demonstrating the specificity of the L-687,414-based procedure.[18] The behavioral effect observed with GlyT1 inhibitors likely results from the increased extracellular level of glycine in the brain and the subsequent displacement of the NMDA glycine site antagonist from its binding site. This L-687,414 based procedure thus represents a useful novel functional method to detect the in vivo activity of GlyT1

inhibitors. In contrast to the microdialysis procedure, which is a highly skilled, time-consuming assay requiring surgery on the tested animal, the L-687,414 based method is comparatively straightforward and possesses sufficient throughput to efficiently guide lead optimization efforts in GlyT1 inhibitor series. We have thus utilized this procedure as a first-line model for the in vivo screening of our benzoylpiperazines.

Despite its attractive in vitro and in vivo efficacy profile, **9** could not be developed further because of a pronounced inhibitory activity measured at the human ether-a-go-go-related gene (hERG) channel (IC_{50} = 0.6 μM, patch-clamp assay). In addition, **9** and close analogues demonstrated a fairly low CNS penetration with measured brain/plasma ratios typically around 0.1.

We report here on our lead optimization effort in the 2-alkoxy-5-methylsulfonebenzoylpiperazine series,[20] addressing the hERG channel and brain penetration issues that culminated in the discovery of RG1678 (**10a**, Figure 3), the first potent and selective GlyT1 inhibitor to have a beneficial effect in schizophrenic patients as shown in a recent phase II clinical trial.[21]

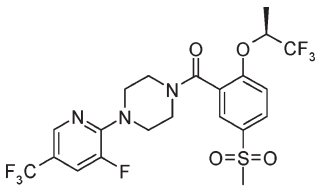

Figure 3. Structure of **10a** (RG1678).

Chemistry

Before describing the synthesis of the GlyT1 inhibitors, we will first discuss the preparation of several noncommercially available benzoic acids as well as *N*-arylpiperazines and *N*-heteroarylpiperazines, which were required as building blocks. The benzoic acids **13a**−**l** were prepared from the known and readily available acid **11**[22] as shown in Scheme 1. **11** was first esterified to provide phenol ester **12** which was subsequently alkylated either under Mitsunobu conditions or by reaction with an alkyl halide or a triflate reagent.

The chiral acids **19** and **19**(+) were prepared from 2-fluorobenzoic acid **14** following the synthetic route described in Scheme 2. Upon treatment with chlorosulfonic acid, **14** underwent a fully regioselective Friedel−Crafts reaction to provide sulfonyl chloride **15** which was subsequently reduced to the sulfinic acid **16**. Reaction of **16** with methyl iodide delivered the methylsulfone methyl ester derivative **17**, which was then saponified to the acid **18**. Finally, the desired chiral acids **19** and **19**(+) were readily obtained upon heating **18** with, respectively, (*rac*)- and (*S*)-1,1,1-trifluoropropan-2-ol[23] in the presence of a mild base such as potassium carbonate. Importantly, this aromatic nucleophilic substitution reaction

Scheme 1. Synthesis of Benzoic Acids **13a**−**l**[a]

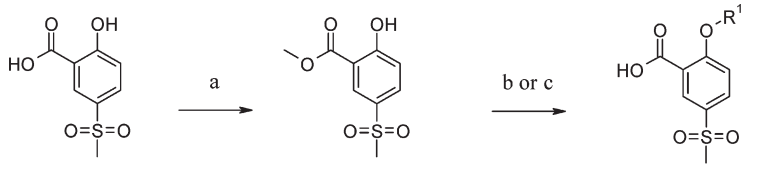

n°	13a	13b	13c	13d	13e	13f	13g	13h	13i	13j	13k	13l
R^1	Et	Benzyl	*n*-Pr	*i*-Bu	*i*-Pr	*c*-C_4H_7	*c*-C_5H_9	*c*-C_6H_{11}	CH_2-*c*-C_6H_{11}	THP-4-yl	CH_2CF_3	$CH_2CH_2NMe_2$
Conditions	b	b	b	b	b	b	b	b	b	b	c	c
Yield	56%	80%	74%	83%	98%	42%	86%	87%	36%	78%	86%	6%

[a] Reagents and conditions: (a) cat. H_2SO_4, MeOH, reflux, 8 days, 89%; (b) R^1OH (1 equiv), di-*tert*-butylazodicarboxylate (1 equiv), triphenylphosphine (1 equiv), THF, room temperature, 24 h, then 2 N NaOH (2 equiv), ethanol, 80 °C, 1 h; (c) R^1X (1.5 equiv), K_2CO_3 (2 equiv), acetone, 70 °C, 22 h, then 2 N NaOH (2 equiv), ethanol, 80 °C, 0.5 h.

Scheme 2. Synthesis of Benzoic Acids **19** and **19**(+)[a]

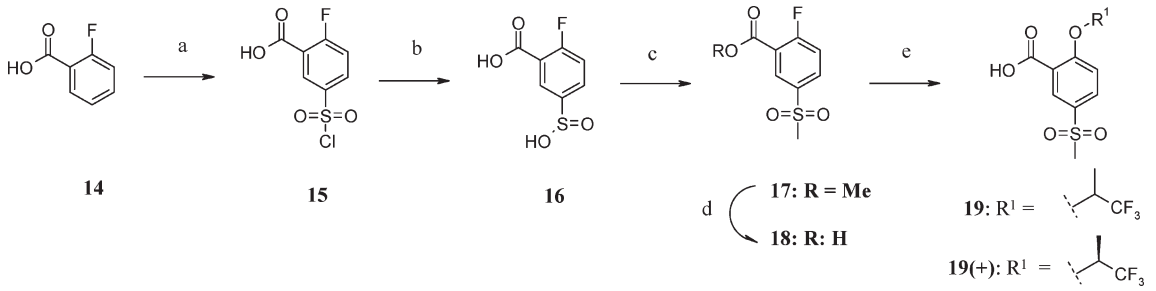

[a] Reagents and conditions: (a) chlorosulfonic acid (10 equiv), 75 °C, overnight, 76%; (b) sodium sulfite (7.5 equiv), water, room temperature, 2 h, 72%; (c) methyl iodide (3.5 equiv), potassium carbonate (3 equiv), room temperature, overnight, 59%; (d) LiOH (1.5 equiv), THF, water, room temperature, 1 h, 85%; (e) *rac*- or (*S*)-1,1,1-trifluoropropan-2-ol (5 equiv), potassium carbonate (3 equiv), dimethylacetamide, 150 °C, 2 h, 40−70%.

Scheme 3. Synthesis of *N*-Aryl-/Heteroarylpiperazines **21a**−**h**[a]

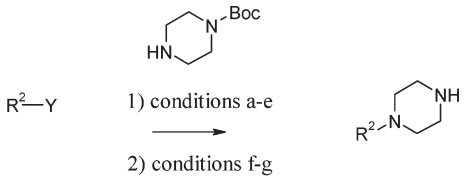

20 **21a-h**

n⁰	21a	21b	21c	21d	21e	21f	21g	21h
R^2								
Conditions	a, f	b, g	b, g	b, g	c, g	d, g	d, f	e, g
Y	F	Br	Cl	Cl	F	Br	Br	I
Yield from **20**	74%	51%	70%	36%	93%	61%	60%	5%

[a] Reagents and conditions: (a) dimethylacetamide, 110 °C, overnight; (b) dimethylacetamide, 150−180 °C in microwave, 10−20 min; (c) potassium carbonate (2 equiv), acetonitrile, reflux, 2 h; (d) tris(dibenzylideneacetone)dipalladium chloroform complex (0.01 equiv), 2-(dicyclohexylphosphino)biphenyl (0.02 equiv), sodium *tert*-butoxide (1.4 equiv), toluene, 80 °C, 12 h, (e) tris(dibenzylideneacetone)dipalladium (0.025 equiv), tri-*o*-tolylphosphine (0.1 equiv), sodium *tert*-butoxide (2.8 equiv), dioxane, 100 °C, 7 h; (f) 4 N HCl (4 equiv), dioxane, 80 °C, overnight; (g) trifluoroacetic acid (5 equiv), dichloromethane, reflux, 2−24 h.

Scheme 4. Synthesis of 2-Piperazin-1-yl-5-trifluoromethylpyrimidine **24**[a]

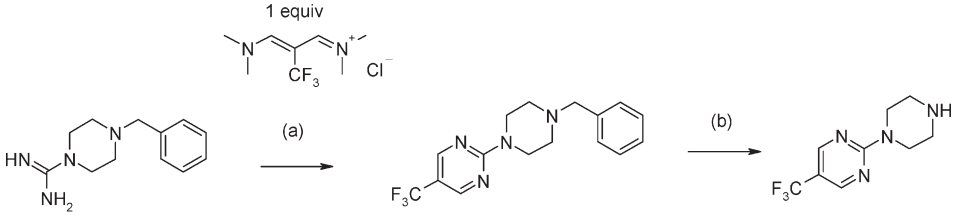

22 **23** **24**

[a] Reagents and conditions: (a) triethylamine (2.4 equiv), acetonitrile, room temperature, 3 h, 94%; (b) H_2 (1 atm), 5% Pd/C, methanol, 60 °C, 2 h, 92%.

proceeded without any erosion of the stereochemical integrity of the chiral center.

The novel *N*-arylpiperazines or *N*-heteroarylpiperazines **21a**−**h** were synthesized upon reaction of *tert*-butyl 1-piperazinecarboxylate with aryl or heteroaryl halides **20** followed by cleavage of the Boc group under acidic conditions (Scheme 3). Hartwig/Buchwald palladium-catalyzed amination conditions were used for the least activated aryl and heteroaryl halides, whereas noncatalyzed thermal conditions were employed for the most activated ones.

Finally, novel 2-piperazin-1-yl-5-trifluoromethylpyrimidine **24** was readily constructed using Yamanaka's methodology[24] involving the condensation of commercial guanidine derivative **22** with (3-dimethylamino-2-trifluoromethylallylidene)dimethylammonium chloride salt (Scheme 4).

2-Alkoxy-5-methylsulfonebenzoylpiperazine derivatives **10a**,**b**, **26**−**54**, **56** were synthesized by employing an amidation reaction between the benzoic acids **13a**−**m**, **19**, **19**(+) and the *N*-arylpiperazines or heteroarylpiperazines **21a**−**p**, **24** (Scheme 5). Phenol **25** was prepared by deprotection of the *O*-benzyl substituted derivative **37** in the presence of iodotrimethylsilane. 3-Methyl-5-trifluoromethylpyridin-2-yl substituted compound **55** was obtained from 3-chloro derivative **56** following a palladium-catalyzed cross-coupling reaction using trimethylaluminum as the methyl donor agent.[25]

Results and Discussion

Starting from **9**, our efforts focused first on the optimization of the alkoxy group. Replacement of the cyclopropylmethoxy moiety with a hydroxyl group (**25**) or with small alkoxy substituents (**26**, **27**) resulted in a dramatic reduction of GlyT1 affinity (Table 1). Pleasingly, the activity was recovered upon increasing the size or the lipophilic bulk of this substituent as seen with the alkoxy (**28**−**30**), cycloalkoxy (**31**−**33**), and fluoroalkoxy (**34**, **35**) derivatives, which all displayed GlyT1 activities in the low nanomolar range. An abrupt drop of potency was, however, observed with more extended substituents such as the cyclohexylmethoxy or benzyloxy groups (**36**, **37**) as well as with groups carrying polar atoms (**38**, **39**), suggesting that substituents at position 2 of the benzoyl motif fit in a size-limited and lipophilic pocket of the GlyT1 receptor. Gratifyingly, all active derivatives, in addition, displayed excellent selectivity versus the GlyT2 isoform (Table 1).

Some of the most potent analogues were selected for further evaluation at the hERG channel and in the L-687,414-induced hyperlocomotion assay in mice (Table 2). Isobutyloxy analogue **29** displayed a similarly high activity at hERG channel compared with initial lead compound **9** (IC_{50} = 0.7 μM) and a comparable in vivo activity (ID_{50} = 2.5 mg/kg). Interestingly, exchange of the elongated alkoxy groups in **9** and **29** with

Scheme 5. Synthesis of 2-Alkoxy-5-methylsulfonebenzoylpiperazines: **10a**,**b** and **25**−**56**[a]

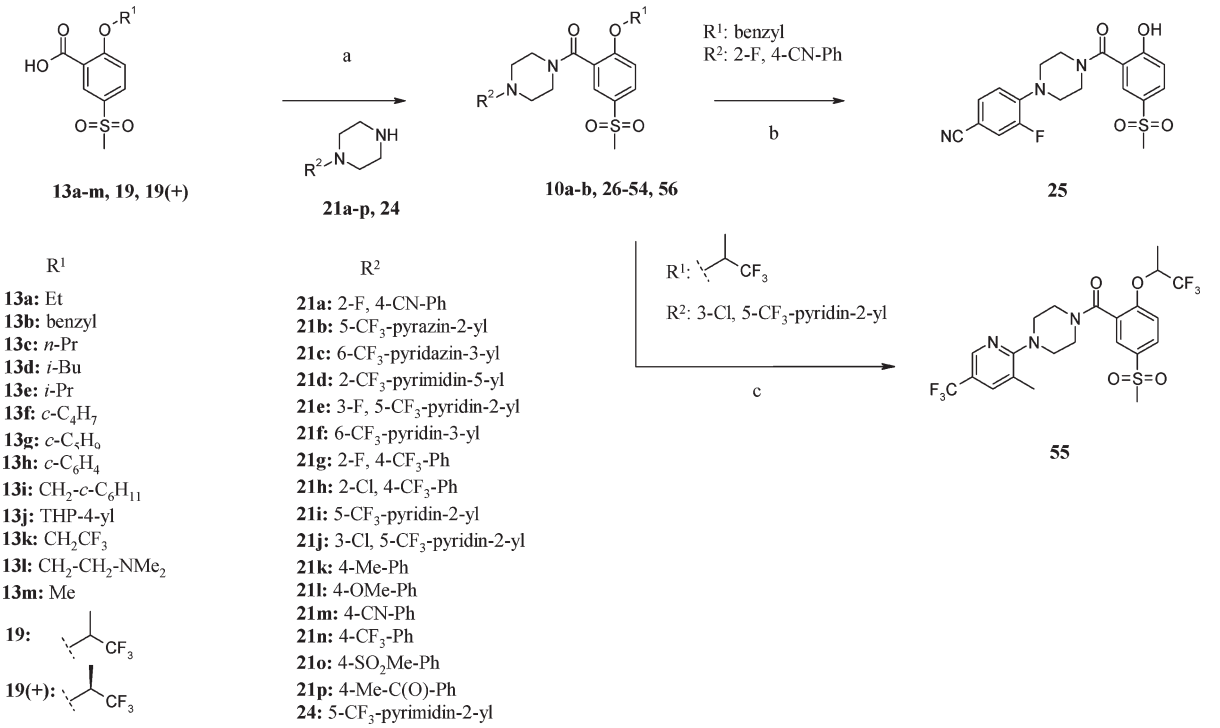

[a] Reagents and conditions: (a) TBTU (1.1 equiv), *i*-Pr_2NEt (5 equiv), DMF, room temperature, overnight, 33−100%; (b) iodotrimethylsilane (4 equiv), acetonitrile, 80 °C, 48 h, 37%; (c) trimethylaluminium (3.6 equiv), tetrakis(triphenylphosphine)palladium (0.24 equiv), THF, 65 °C, 68 h, 46%.

Table 1. In Vitro Inhibitory Activity of **9** and **25**−**39** at hGlyT1 and hGlyT2

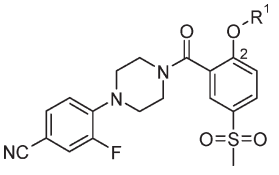

compd	R^1	EC_{50}, μM[a] hGlyT1	hGlyT2
9	CH_2-*c*-Pr	0.016	> 30
25	H	> 10	> 30
26	Me	9.80	> 30
27	Et	0.59	> 30
28	*n*-Pr	0.034	> 30
29	*i*-Bu	0.010	> 30
30	*i*-Pr	0.070	> 30
31	*c*-C_4H_7	0.018	> 30
32	*c*-C_5H_9	0.012	> 30
33	*c*-C_6H_{11}	0.008	> 30
34	CH_2CF_3	0.028	> 30
35	$CH(CH_3)CF_3$	0.044	> 30
36	CH_2-*c*-C_6H_{11}	0.39	> 30
37	benzyl	1.61	> 30
38	THP-4-yl	0.50	> 30
39	$CH_2CH_2NMe_2$	> 10	> 30

[a] EC_{50} values are the average of at least two independent experiments.

shorter substituents such as isopropyloxy (**30**), trifluoroethoxy (**34**), and trifluoroisopropyloxy (**35**) induced a significant decrease of hERG inhibitory activity (IC_{50} = 3.3, 2, and 3 μM, respectively). In the case of **30** and **34**, however, a concomitant drop of in vivo activity (ID_{50} = 8 mg/kg for **30** and 7 mg/kg for **34**) was observed. In contrast, the reduction in hERG activity with the trifluoroisopropyloxy derivative **35** was found to be accompanied by an improvement in in vivo efficacy reaching an ID_{50} of 1 mg/kg. In pharmacokinetics studies, all compounds in Table 2 exhibited equivalent plasma exposures after oral dosing but different brain concentrations and therefore different brain/plasma ratios. Overall, in vivo activity seemed to correlate quite well with the brain penetration, with the highest efficacy obtained with compound **35** which displayed a superior brain/plasma ratio (0.25) compared to the other alkoxy derivatives examined (Table 2). In summary, because of its beneficial effect on CNS penetration plus in vivo and hERG profiles, the trifluoroisopropyloxy group emerged as the best substituent among the set of alkoxy residues investigated. This group thus constituted a highly favored substituent at the 2-position in the benzoylpiperazine class.

With the preferred trifluoroisopropyloxy group kept in place at position 2, our effort next focused on the optimization of the western aromatic region. In agreement with the preliminary SAR results obtained on our initial HTS hit **8**,[16] the introduction of electron-donating groups like methyl (**40**) or methoxy (**41**) in the para position of the aromatic system resulted in weakly active GlyT1 inhibitors. Higher affinities were obtained with analogues carrying strong EWGs such as nitrile (**42**), trifluoromethyl (**43**), methyl sulfone (**44**), or methyl ketone (**45**) functions (Table 3). In particular, the best in vitro results were seen with the nitrile (**42**) and trifluoromethyl (**43**) derivatives which showed respectively a GlyT1 affinity of 21 and 30 nM. Keeping the *p*-trifluoromethyl group in place, a significant improvement in GlyT1 potency was detected upon the introduction of a small EWG like fluorine in the ortho position as observed with compound **46** (13 nM).

Table 2. Activity of **9**, **29**, **30**, **34**, **35** at the hERG Channel and in the L-686,414-Induced Hyperlocomotion Assay in Mouse

					mouse		
compd	hERG IC_{50}, μM[a]	clogP[b]	PSA, Å^2 [c]	reversal of L-687,414-induced hyperlocomotion in mouse ID_{50}, mg/kg[d]	C_{max} plasma, ng/mL[e]	C_{max} brain, ng/mL[e]	brain/plasma[e]
9	0.6	2.64	80	3.0	3870	387	0.10
29	0.7	3.13	80	2.5	2900	460	0.16
30	3.3	2.51	80	8.0	3143	220	0.07
34	2.0	2.64	80	7.0	3000	240	0.08
35	3.0	2.77	80	1.0	3100	775	0.25

[a] Patch clamp assay. IC_{50} values are the average of at least two independent experiments. [b] Calculated lipophilicity.[26] [c] Polar surface area calculated with Moloc.[27] [d] Compound given orally, $n = 8$. [e] Compound given orally at a dose of 10 mg/kg, $n = 2$.

However, introduction of a larger halogen atom such as chlorine (**47**) at this position resulted in a sharp drop of activity (200 nM). Further in vitro and in vivo characterization revealed that the trifluoromethyl derivatives **43** and **46** had more favorable profiles than the corresponding nitrile analogues **42** and **35**. First, with brain/plasma ratios of about 1, **43** and **46** demonstrated a much-improved CNS penetration. Knowing that PSA might be an important parameter that limits blood−brain barrier permeation, we hypothesized that this result might be attributed to their lower polar surface area (PSA = 59 Å^2 vs 80 Å^2). We applied the Roche automatic SAR analyzer (ROSARA),[28] a proprietary program designed to study potential correlation between a given property (i.e., brain penetration in this case) and numerous calculated (e.g., clogP or PSA) or measured (e.g., GlyT1 EC_{50}, solubility or permeability) descriptors. In fact, ROSARA revealed that the measured CNS penetration in our series could be very well predicted by using solely PSA and clogP as descriptors (Figure 4).

In addition to their superior CNS penetration, the trifluoromethylated analogues **43** and **46** showed significantly lower inhibitory activities at the hERG channel compared to the corresponding more polar nitrile analogues **42** and **35** (IC_{50} = 10 and 6.9 μM vs 1.2 and 3 μM). This result is quite remarkable because it is well recognized that, on the contrary, a reduction of compound lipophilicity in a chemical series is often associated with a decrease of hERG channel affinity.[29] We hypothesize that the high hERG inhibition observed with the nitrile derivatives is due to a specific H-bonding interaction of the cyano group with a key amino acid residue in the pore region of the hERG channel.[30] The superior in vitro and brain/plasma ratios demonstrated by the trifluoromethyl substituted derivatives prompted us to focus our subsequent optimization effort specifically on this class of compounds. Starting from **43**, we set out to further improve the hERG selectivity profile. Toward this end, analogues with increased polarity, obtained by exchanging the western aromatic nucleus of **43** with heteroaromatic systems such as pyridines **48** and **49**, pyrazine **50**, pyrimidines **51** and **52**, and pyridazine **53**, were investigated (Table 3). Our strategy proved successful because pyridine derivative **48**, displaying a favorable GlyT1 affinity (IC_{50} = 37 nM), showed a 2-fold reduction in hERG activity (IC_{50} = 20 μM) over the parent compound **43**. With compound **48**, we thus achieved for the first time a high level of selectivity against the hERG channel, reaching over 500-fold. However, because of its increased polar surface area (PSA = 69 Å^2) and reduced lipophilicity (clogP = 2.82), **48** exhibited a reduced CNS penetration (brain/plasma: 0.2 vs 1.1 for **43**) and accordingly, a lower in vivo activity (ID_{50} = 5 mg/kg) in the L-687,414-induced hyperlocomotion assay. Shifting the pyridinyl ring nitrogen to the adjacent position to afford **49** provided a compound with reduced GlyT1 potency (IC_{50} = 80 nM). Similarly, a decrease of GlyT1 activity was unfortunately observed with the pyrazine, pyrimidine, and pyridazine derivatives **50**−**53**. It is, however, interesting to note that these more polar heteroaryl derivatives having clogP values ranging from 1.83 to 1.96 were practically devoid of any hERG activity (IC_{50} > 40 μM). Thus, the structure−hERG activity relationship described in this compound class clearly illustrates that the exchange of an aryl group by heteroaryl systems can be a very powerful medicinal chemistry strategy to control hERG affinity in chemical series. Starting from pyridine derivative **48**, our next step was to improve the CNS penetration and in vivo potency while retaining the excellent selectivity profile against the hERG channel. The well-documented beneficial effect of fluorine atom insertion on CNS penetration of biologically active molecules[31] led us to consider analogues to pyridine compound **48** incorporating an extra fluorine atom. Additionally, we reasoned that this modification would probably not affect the selectivity toward the hERG channel, since a hydrogen to fluorine exchange in molecules generally results in only a moderate increase of lipophilicity.[32]

The tolerance of the fluorine atom for GlyT1 activity observed in the ortho aryl position in derivative **46** led us to prepare the 3-F, 5-CF_3-pyridyl substituted compound **54**. As we expected, **54** showed a very good affinity at GlyT1 transporter (IC_{50} = 40 nM), comparable to the potency obtained for the parent pyridine compound **48**. Gratifyingly, as we anticipated, **54** demonstrated an improved brain penetration (brain/plasma: 0.5 vs 0.2 for **48**) and consequently a superior in vivo activity in the L-687,414 mouse assay with an ID_{50} reaching 1 mg/kg after oral administration. Moreover, as desired, the introduction of a fluorine atom into **48** did not impact negatively on the selectivity against the hERG channel (500-fold selectivity, IC_{50} = 20 μM). In summary, the hydrogen to fluorine exchange performed at position 3 on the pyridine ring of compound **48** delivered a potent GlyT1 inhibitor **54** displaying an excellent hERG selectivity combined with a robust CNS penetration and in vivo potency. The alternative exchanges examined at that position, hydrogen vs methyl (**55**) and vs chlorine (**56**), met with much less success, illustrating once again the unique beneficial effect a fluorine group may have on compound properties. Indeed, the methyl analogue **55** had a significantly lower GlyT1 affinity (IC_{50} = 80 nM) and the chloro derivative **56**, while potent at GlyT1 (IC_{50} = 30 nM), showed a reduced in vivo activity (ID_{50} = 4 mg/kg) as well as a decreased selectivity vs the hERG channel (300-fold), a result likely due to its higher lipophilicity (clogP = 3.57 vs 3.00 for **54**). Compound **54**, existing as a racemic mixture, was subsequently separated by chiral phase HPLC to provide the two enantiomers **10a** ((*S*)-enantiomer) and **10b** ((*R*)-enantiomer). **10a** was found positively differentiated over its enantiomer **10b** by its higher in vitro GlyT1

Table 3. In Vitro and in Vivo Profiles of **40**−**56** and **10a**,**b**

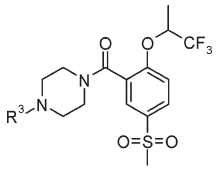

Compound	R^3	GlyT1 EC_{50}, μM[a]	GlyT2 EC_{50}, μM[a]	hERG IC_{50}, μM[b]	clogP[c]	PSA Å^2[d]	Reversal of L-687,414-induced hyperlocomotion in mouse ID_{50}, mg/kg[e]	Brain /plasma in mouse[f]
40		0.31	> 30	–	3.24	59	–	–
41		0.43	> 30	–	2.76	68	–	–
42		0.021	> 30	1.2	2.57	80	3.0	0.04
43		0.03	> 30	10	3.92	59	2.0	1.10
44	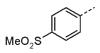	0.10	> 30	–	1.53	90	–	–
45		0.091	> 30	–	2.49	75	–	–
46		0.013	> 30	6.9	4.13	59	2.0	1.15
47		0.20	> 30	–	4.70	59	–	–
48		0.037	24.2	20	2.82	69	5.0	0.20
49		0.080	> 30	–	2.82	70	–	–
50		0.11	> 30	> 40	1.96	79	–	–
51		0.10	> 30	> 40	1.96	79	–	–
52		0.53	> 30	> 40	1.96	79	–	–
53		0.90	> 30	–	1.83	82	–	–
54		0.040	> 30	20	3.00	69	1.0	0.50
55		0.080	29	–	3.32	68	–	–
56		0.030	> 30	10	3.57	69	4.0	–
10a	(*S*)- enantiomer of **54**	0.030	> 30	17	3.00	69	0.5	0.50
10b	(*R*)- enantiomer of **54**	0.057	> 30	28	3.00	69	3.0	–

[a] EC_{50} values are the average of at least two independent experiments. [b] Patch clamp assay. IC_{50} values are the average of at least two independent experiments. [c] Calculated lipophilicity.[26] [d] Polar surface area calculated with Moloc.[27] [e] Compound given orally, $n = 8$. [f] Compound given orally at the dose of 10 mg/kg, $n = 2$.

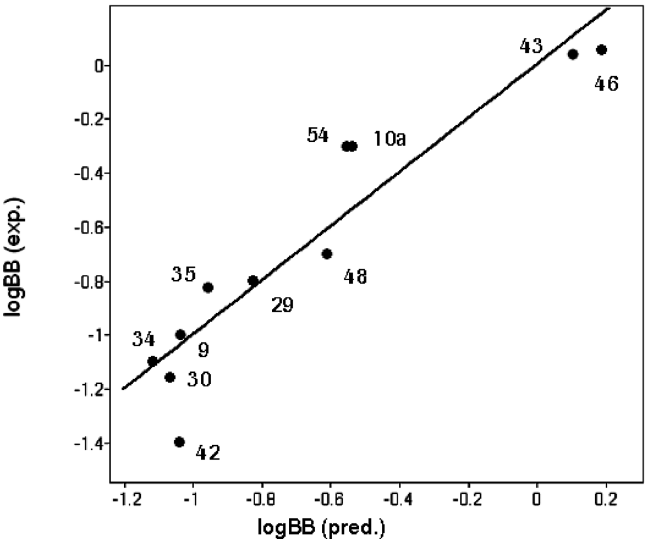

Figure 4. Correlation of experimental vs calculated log BB (log of brain/plasma ratio) using the Roche Automatic SAR analyzer (ROSARA). The model relies solely on two descriptors: clogP and PSA. The line of identity is shown in black. A linear regression leads to the following parameters: $n = 11$; $r^2 = 0.875$; $q^2 = 0.845$.

Table 4. Pharmacokinetic Properties of **10a** in Rat and Cynomolgus Monkey

parameter	species	
	rat[h]	cynomolgus monkey[h]
iv dose (mg/kg)[a]	2	0.5
CL ((mL/min)/kg)[b]	4.32 (±25%)	3.62 (±9%)
V_{dss} (L/kg)[c]	3.58 (±14%)	1.98 (±8%)
po dose (mg/kg)[d]	3	2.8
C_{max} (ng/mL)	721 (±13%)	517 (±38%)
$AUC_{0-\infty}$ (ng·h/mL)[e]	8670 (±16%)	7230 (±2%)
$T_{1/2}$ (h) terminal	5.8 (±25%)	6.4 (±8%)
T_{max} (h)	1	5.5 (±64%)
F (%)[f]	78 (±20%)	56 (±3%)
brain/plasma	0.7	
PPB (% unbound)[g]	3	3

[a] iv formulations. Rat: NMP/hydroxypropyl γ-cyclodextrin. Monkey: 30% captisol. [b] Total plasma clearance. [c] Volume of distribution. [d] po formulation. Tween-80, methylparaben, propylparaben, and hydroxyethylcellulose. [e] Area under the curve extrapolated to infinity. [f] Oral bioavailability. [g] Plasma protein binding. [h] $n = 2$. Mean values (±CV%).

activity ($IC_{50} = 30$ nM) and superior in vivo efficacy in the L-687,414-induced hyperlocomotion assay, reaching for the first time an ID_{50} as low as 0.5 mg/kg po while hERG activity still resided in a favorable range ($IC_{50} = 17\ \mu M$). Additional profiling revealed that **10a** had an excellent selectivity profile against the GlyT2 isoform ($IC_{50} > 30\ \mu M$) and toward a panel of 86 targets including transmembrane and soluble receptors, enzymes, ion channels, and monoamine transporters (<41% inhibition at 10 μM was measured for all targets).[33] Although **10a**, a nonbasic compound ($pK_a < 2$), showed low aqueous solubility (1 μg/mL with crystalline material at pH 6.5), it exhibited a satisfactory solubility profile in both fasted state simulated intestinal fluid (FaSSIF) (20 μg/mL) and fed state simulated intestinal fluid (FeSSIF) (60 μg/mL). **10a** showed, in addition, excellent membrane permeability as measured in the parallel artificial membrane permeation assay (PAMPA) ($P_e = 3.2 \times 10^{-6}$ cm/s).[34] In vivo pharmacokinetic studies in rat and monkey (Table 4) revealed that **10a** had, in both species, a low plasma clearance, an intermediate volume of distribution, a good oral bioavailability (78% for rat, 56% for monkey), and a favorable terminal half-life (5.8 h for rat, 6.4 h for monkey). The plasma protein binding was high in the two preclinical species (97%) and in human (98%). The CNS penetration of **10a** in rat (brain/plasma = 0.7) was better than that in mouse (brain/plasma = 0.5). Finally, compound **10a** did not significantly inhibit the major drug metabolizing CYP450 enzymes 3A4, 2D6, 2C9, 2C19, 1A2 (all IC_{50} values above 24 μM) and was without activity in genotoxicity assays (Ames and MNT tests).

The excellent data obtained with **10a** prompted us to evaluate the effect of this compound on the extracellular level of glycine in rat striatum in a microdialysis study (Figure 5). Gratifyingly, at an oral dose of 10 mg/kg, **10a** produced a robust and sustained increase of glycine levels (2.3-fold over basal levels at 180 min). The lack of effect on the striatal extracellular levels of D/L-serine (data not shown) indicated that this compound did not affect other neutral amino acid transporters and provided in vivo evidence of its selectivity for the GlyT1 transporter.

Conclusion

In summary, chemical optimization in the class of benzoylpiperazines has led to the discovery of compound **10a**, a highly

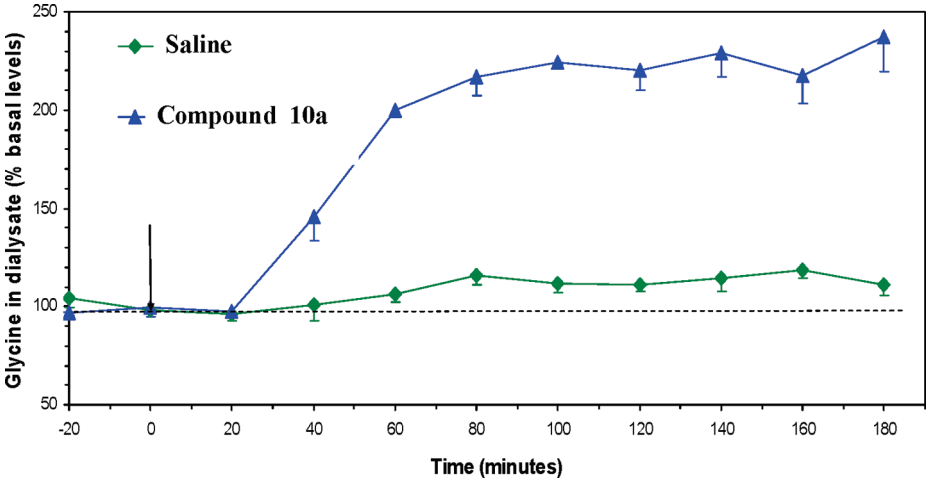

Figure 5. Effect of **10a** on the extracellular level of glycine in rat striatum at 10 mg/kg po measured by microdialysis. Data are the mean ± SEM ($n = 3$).

potent and selective GlyT1 inhibitor exhibiting excellent pharmacokinetic and in vivo efficacy profiles in nonhuman species. On this basis, **10a** advanced into clinical trials in healthy subjects and in schizophrenic patients. F. Hoffmann-La Roche recently reported positive phase II results with **10a** for the treatment of negative symptoms, a core clinical feature of schizophrenia where there are currently no effective therapies. The complete biological characterization of **10a** will be reported in further detail in forthcoming publications.

Experimental Section

Chemistry. General. All solvents and reagents were obtained from commercial sources and were used as received. All reactions were followed by TLC (TLC plates F254, Merck) or LCMS (liquid chromatography−mass spectrometry) analysis. Proton NMR spectra were obtained on Bruker 300 or 400 MHz instrument with chemical shifts (δ in ppm) reported relative to tetramethylsilane as internal standard. NMR abbreviations are as follows: s, singlet; d, doublet; t, triplet; q, quadruplet; quint, quintuplet; sext, sextuplet; hept, heptuplet; m, multiplet; br, broadened. Purity was analyzed by reverse phase HPLC and for specific compounds by elemental analysis. HPLC was performed on Finnigan LTQ (Thermo Fisher Scientific) and Agilent RRLC 1200 equipment. The column was Agilent XDB C15, 30 mm × 4.6 mm, 3.5 μm. Analytical conditions were as folllows: Gradient used was from 5% to 95% acetonitrile in water containing 0.1% trifluoroacetic acid in 3 min. Flow was 4.5 mL/min. UV detector was DAD, 190−400 nm. Sample solvent was in water/acetonitrile (8/2). The UV detection was an averaged signal from wavelengths of 190−400 nm. Elemental analyses were performed by Solvias AG (Mattenstrasse, Postfach, CH-4002 Basel, Switzerland). Column chromatography was carried out on silica gel 60 (32−60 mesh, 60 Å) or on prepacked columns (Isolute Flash Si). Mass spectra were recorded on an SSQ 7000 (Finnigan-MAT) spectrometer for electron impact ionization. The purities of final compounds **10a**,**b** and **25**−**56** as measured by HPLC or elemental analysis method were found to be above 95%.

Detailed Description. 5-Chlorosulfonyl-2-fluorobenzoic Acid (15). To chlorosulfonic acid (238 mL, 3.5 mol, 10 equiv) cooled to 0 °C was added portionwise 2-fluorobenzoic acid **14** (50 g, 0.35 mol). After complete addition, the yellow solution was allowed to warm to room temperature, then heated to 75 °C overnight. The reaction mixture was cooled to room temperature and then added dropwise to ice (1.5 L). The white precipitate was filtered, washed with water, and dried in vacuo to afford the desired product as a white solid (63 g, 76%). ^{1}H NMR (300 MHz, $CDCl_3$) δ 8.76 (dd, J = 6.3, 2.7 Hz, 1H), 8.29 (m, 1H), 7.47 (t, J = 9.3 Hz, 1H). MS (EI) m/e: 236.8(M − H).

2-Fluoro-5-sulfinobenzoic Acid (16). To a solution of sodium sulfite (250 g, 1.98 mol, 7.5 equiv) in water (1 L) was added portionwise during 20 min chlorosulfonyl-2-fluorobenzoic acid **15** (63 g, 0.264 mol). The reaction mixture was stirred at room temperature for 2 h, then cooled to 0 °C and acidified with 20% sulfuric acid (~230 mL) to pH 2. Water was evaporated, and methanol (600 mL) was added. The mixture was stirred overnight and filtered and the filtrate was then concentrated and dried over sodium sulfate to afford the desired product as a white solid (39 g, 72%). ^{1}H NMR (300 MHz, DMSO-d_6) δ 7.73 (dd, J = 7.6, 2.2 Hz, 1H), 7.36 (m, 1H), 6.95 (dd, J = 10.4, 8.2, Hz, 1H). MS (EI) m/e: 203.0 (M − H).

2-Fluoro-5-methanesulfonylbenzoic Acid Methyl Ester (17). To a solution 2-fluoro-5-sulfinobenzoic acid **16** (19.5 g, 95.3 mmol) in DMF (166 mL) was added potassium carbonate (39.5 g, 286 mmol, 3 equiv) and then methyl iodide (20.8 mL, 333 mmol, 3.5 equiv). The reaction mixture was stirred at room temperature overnight. Then DMF (100 mL) was removed in vacuo, and water (100 mL) was added followed by ethyl acetate (100 mL). The aqueous phase was extracted twice. The combined organic phases were dried over sodium sulfate, then concentrated in vacuo to provide the desired product as a light-yellow solid (13.1 g, 59%) which was used in the next reaction without further purification. ^{1}H NMR (300 MHz, $CDCl_3$) δ 8.55 (dd, J = 6.6, 2.4 Hz, 1H), 8.13 (m, 1H), 7.36 (dd, J = 9.9, 9.0 Hz, 1H), 3.98 (s, 3H), 3.09 (s, 3H). MS (EI) m/e: 250.1 $(M + NH_4)^+$.

2-Fluoro-5-methanesulfonylbenzoic Acid (18). To a solution of 2-fluoro-5-methanesulfonylbenzoic acid methyl ester **17** (18 g, 77.3 mmol) in THF (360 mL) and water (360 mL) was added lithium hydroxide monohydrate (4.9 g, 116 mmol, 1.5 equiv). The reaction mixture was stirred at room temperature for 1 h. Then THF was distilled in vacuo and 1 N HCl was added to reach pH 2. The mixture was extracted with diethyl ether (2 × 60 mL). The combined organic phases were dried over sodium sulfate, then concentrated in vacuo. The crude material was triturated with diisopropyl ether to provide, after filtration and drying, the desired product as a white solid (14.4 g, 85%). ^{1}H NMR (300 MHz, DMSO-d_6) δ 13.8 (br s, 1H), 8.36 (dd, J = 6.9, 2.4 Hz, 1H), 8.20 (m, 1H), 7.63 (dd, J = 10.5, 8.7 Hz, 1H), 3.30 (s, 3H). MS (EI) m/e: 235.9 $(M + NH_4)^+$.

***rac*-5-Methanesulfonyl-2-(2,2,2-trifluoro-1-methylethoxy)benzoic Acid (19).** A suspension containing **18** (0.20 g, 0.92 mmol), *rac*-1,1,1-trifluoropropan-2-ol (0.40 mL, 4.58 mmol, 5 equiv), and potassium carbonate (0.38 g, 2.75 mmol, 3 equiv) in dimethylacetamide (5 mL) was stirred at 150 °C for 2 h, then cooled to room temperature and concentrated in vacuo. The residue was diluted with water (5 mL) and acidified with 1 N HCl to pH 2. The precipitate was filtered, washed with water, and dried in vacuo to afford the desired product as a white solid (0.11 g, 40%). ^{1}H NMR (300 MHz, $CDCl_3$) δ 8.63 (d, J = 2.4 Hz, 1H), 8.13 (dd, J = 8.7, 2.4 Hz, 1H), 7.21 (d, J = 8.7 Hz, 1H), 4.94 (m, 1H), 3.09 (s, 3H), 1.66 (d, J = 6.5 Hz, 3H). MS (EI) m/e: 311.1 (M − H).

(*S*)-5-Methanesulfonyl-2-(2,2,2-trifluoro-1-methylethoxy)benzoic Acid (19(+)). Preparation followed the same procedure as for **19** from **18** and (*S*)-1,1,1-trifluoro-propan-2-ol[23] (70% yield, white solid). $[\alpha]_D^{20}$ +16.9° (c 1.01, MeOH). ^{1}H NMR (300 MHz, $CDCl_3$) δ 8.63 (d, J = 2.4 Hz, 1H), 8.13 (dd, J = 8.7, 2.4 Hz, 1H), 7.21 (d, J = 8.7 Hz, 1H), 4.94 (m, 1H), 3.09 (s, 3H), 1.66 (d, J = 6.5 Hz, 3H). MS (EI) m/e: 311.1 (M − H). The optical purity was determined by chiral HPLC of the corresponding methyl ester (obtained by refluxing acid in methanol with the presence of catalytic amount of sulfuric acid) using a Chiralpack AD column (flow 1 mL/min, pressure of 25 bar, detection at 254 nm) and using heptane/isopropanol, 80:20, as eluant: retention time of 22.9 min, ee of >99%.

1-(3-Fluoro-5-trifluoromethylpyridin-2-yl)piperazine (21e). A mixture of 2,3-difluoro-5-trifluoromethylpyridine (21 g, 115 mmol), *tert*-butyl 1-piperazinecarboxylate (23.1 g, 120 mmol, 1.05 equiv), and potassium carbonate (31.7 g, 229 mmol, 2 equiv) in acetonitrile (315 mL) was refluxed for 2 h. The reaction mixture was then cooled to room temperature and filtered, and the filtrate was concentrated in vacuo. The solid was dissolved in ethyl acetate (250 mL). The solution was washed once with water (100 mL) and with 1% citric acid solution (3 × 100 mL), dried over sodium sulfate, filtered, and concentrated in vacuo to afford 4-(3-fluoro-5-trifluoromethylpyridin-2-yl)piperazine-1-carboxylic acid *tert*-butyl ester as a white solid (37.5 g). This material was dissolved in dichloromethane (376 mL), and trifluoroacetic acid (41.1 mL, 537 mmol, 5 equiv) was added. The resulting mixture was refluxed for 16 h and then cooled to room temperature and concentrated in vacuo. The residue was diluted with water (450 mL), basified with 5 N NaOH, and extracted with dichloromethane (3 × 50 mL). The combined extracts were washed with brine (50 mL), dried over sodium sulfate, filtered, and concentrated in vacuo to afford the desired compound as a light-yellow solid (26.4 g, 93%). ^{1}H NMR (300 MHz, $CDCl_3$) δ 8.22 (d, J = 1.9 Hz, 1H), 7.37 (dd, J = 13.5, 2.0 Hz, 1H), 3.63 (t, J = 4.8 Hz, 4H), 2.99 (t, J = 5.1 Hz, 4H). MS (EI) m/e: 250.2 $(M + H)^+$.

***rac*-4-(3-Fluoro-5-trifluoromethylpyridin-2-yl)piperazin-1-yl]-[5-methanesulfonyl-2-(2,2,2-trifluoro-1-methylethoxy)phenyl]-methanone (54). General Procedure C.** To a solution of **19**

(14 g, 44.8 mmol) in DMF (140 mL) was added successively TBTU (16.2 g, 49.3 mmol, 1.1 equiv), *N*-ethyldiisopropylamine (38.4 mL, 224.2 mmol, 5 equiv), and **21e** (13.4 g, 53.8 mmol, 1.2 equiv). The reaction mixture was stirred overnight at room temperature, then was concentrated in vacuo, and the residue was dissolved with ethyl acetate (150 mL). The mixture was washed with water (2 × 200 mL) and saturated sodium bicarbonate solution (2 × 150 mL). The aqueous phase was extracted with ethyl acetate (1 × 100 mL). The combined organic phases were dried over sodium sulfate, filtered, and concentrated in vacuo. The crude material was taken up in ethanol (150 mL), and the mixture was heated to 80 °C and then allowed to cool to room temperature and stirred for 3 h. The precipitate was filtered, washed with a small amount of ethanol, and dried in vacuo to afford the desired compound as a white solid (19.9 g, 82%). ^{1}H NMR (400 MHz, $CDCl_3$) δ 8.25 (s broad, 1H), 7.98 (dd, J = 8.6, 2.4 Hz, 1H), 7.95 (br s, 0.3H), 7.91 (d, J = 2.4 Hz, 0.7 H), 7.43 (dd, J = 13.2, 1.6 Hz, 1H), 7.14 (d, J = 8.9 Hz, 0.7H), 7.10 (d, J = 8.9 Hz, 0.3 H), 4.89−4.75 (m, 1H), 4.00−3.84 (m, 2H), 3.81−3.68 (m, 2H), 3.67−3.54 (m, 2H), 3.48−3.28 (m, 2H), 3.07 (s, 3H), 1.6 (d, J = 6.5 Hz, 0.9H), 1.54−1.50 (m, 2.1 H) as a 7:3 mixture of two rotamers. MS (EI) m/e: 544.3 $(M + H)^+$. HPLC: retention time of 1.86 min, >98% pure.

(*S*)-4-(3-Fluoro-5-trifluoromethylpyridin-2-yl)piperazin-1-yl]-[5-methanesulfonyl-2-(2,2,2-trifluoro-1-methylethoxy)phenyl]-methanone (10a) and (*R*)-4-(3-Fluoro-5-trifluoromethylpyridin-2-yl)piperazin-1-yl][5-methanesulfonyl-2-(2,2,2-trifluoro-1-methylethoxy)phenyl]methanone (10b). 54 (530 mg, 0.975 mmol) was separated on a preparative Chiralpack AD column (flow of 35 mL/min, pressure of 15 bar, detection at 254 nm) using heptane/isopropanol, 80:20, as eluant to afford (*S*)-enantiomer **10a** (191 mg, 36% yield, first eluting product, retention time of 110 min) and (*R*)-enantiomer **10b** (197 mg, 37% yield, second eluting product, retention time of 145 min).

10a: white solid, $[\alpha]_D^{20}$ −0.32° (*c* 0.95, $CHCl_3$). ^{1}H NMR (400 MHz, $CDCl_3$) δ 8.25 (s broad, 1H), 7.98 (dd, J = 8.6, 2.4 Hz, 1H), 7.95 (br s, 0.3H), 7.91 (d, J = 2.4 Hz, 0.7 H), 7.43 (dd, J = 13.2, 1.6 Hz, 1H), 7.14 (d, J = 8.9 Hz, 0.7H), 7.10 (d, J = 8.9 Hz, 0.3 H), 4.89−4.75 (m, 1H), 4.00−3.84 (m, 2H), 3.81−3.68 (m, 2H), 3.67−3.54 (m, 2H), 3.48−3.28 (m, 2H), 3.07 (s, 3H), 1.6 (d, J = 6.5 Hz, 0.9H), 1.54−1.50 (m, 2.1 H) as a 7:3 mixture of two rotamers. MS (EI) m/e: 544.3 $(M + H)^+$. Anal. Calcd for $C_{21}H_{20}F_7N_3O_4S$: C, 46.41; H, 3.71; N, 7.73; S, 5.90; F, 24.47. Found: C, 46.21; H, 3.63; N, 7.86; S, 6.07; F, 24.42. HPLC, analytical Chiralpack AD column (flow 1 mL/min, pressure of 25 bar, detection at 254 nm) using heptane/isopropanol, 80:20, as eluant: retention time of 17.4 min, ee of >99%. HPLC: retention time of 1.86 min, >98% pure.

10b: white solid, $[\alpha]_D^{20}$ +0.7° (*c* 1, $CHCl_3$). ^{1}H NMR (400 MHz, $CDCl_3$) δ 8.25 (s broad, 1H), 7.98 (dd, J = 8.6, 2.4 Hz, 1H), 7.95 (br s, 0.3H), 7.91 (d, J = 2.4 Hz, 0.7 H), 7.43 (dd, J = 13.2, 1.6 Hz, 1H), 7.14 (d, J = 8.9 Hz, 0.7H), 7.10 (d, J = 8.9 Hz, 0.3 H), 4.89−4.75 (m, 1H), 4.00−3.84 (m, 2H), 3.81−3.68 (m, 2H), 3.67−3.54 (m, 2H), 3.48−3.28 (m, 2H), 3.07 (s, 3H), 1.6 (d, J = 6.5 Hz, 0.9H), 1.54−1.50 (m, 2.1 H) as a 7:3 mixture of two rotamers. MS (EI) m/e: 544.3 $(M + H)^+$. HPLC, analytical Chiralpack AD column (flow 1 mL/min, pressure of 25 bar, detection at 254 nm) using heptane/isopropanol, 80:20, as eluant: retention time of 22.0 min, ee of >99%. HPLC: retention time of 1.86 min, >98% pure.

Asymmetric Synthesis of 10a. Preparation followed procedure C from **21e** and **19**(+) (78% yield, white solid). $[\alpha]_D^{20}$ −0.32° (*c* 0.95, $CHCl_3$). ^{1}H NMR (400 MHz, $CDCl_3$) δ 8.25 (s broad, 1H), 7.98 (dd, J = 8.6, 2.4 Hz, 1H), 7.95 (br s, 0.3H), 7.91 (d, J = 2.4 Hz, 0.7 H), 7.43 (dd, J = 13.2, 1.6 Hz, 1H), 7.14 (d, J = 8.9 Hz, 0.7H), 7.10 (d, J = 8.9 Hz, 0.3 H), 4.89−4.75 (m, 1H), 4.00−3.84 (m, 2H), 3.81−3.68 (m, 2H), 3.67−3.54 (m, 2H), 3.48−3.28 (m, 2H), 3.07 (s, 3H), 1.6 (d, J = 6.5 Hz, 0.9H), 1.54−1.50 (m, 2.1 H) as a 7:3 mixture of two rotamers. MS (EI) m/e: 544.3 $(M + H)^+$. Anal. Calcd for $C_{21}H_{20}F_7N_3O_4S$: C, 46.41; H, 3.71; N, 7.73; S, 5.90; F, 24.47. Found: C, 46.21; H, 3.63; N, 7.86; S, 6.07; F, 24.42. HPLC, analytical Chiralpack AD column (flow of 1 mL/min, pressure of 25 bar, detection at 254 nm) using heptane/isopropanol, 80:20, as eluant: retention time of 17.4 min, ee of >99%.

hGlyT1 Uptake Inhibition Assay. Mammalian CHO cells (Flp-in-CHO) stably expressing hGlyT1b cDNA were maintained in monolayer culture at 37 °C in humidified air with 5% CO_2 in nutrient mixture F-12 containing 10% fetal calf serum, 1% penicillin−streptomycin, 600 μg/mL hygromicin, and 1 mM glutamine. On day 1 of the glycine uptake experiments, cells were plated at a density of 40 000 cells/well in complete F-12 medium without hygromycin in 96-well culture plates. On day 2, the medium was aspirated and the cells were washed twice with uptake buffer (150 mM NaCl, 10 mM Hepes-Tris, pH 7.4, 1 mM $CaCl_2$, 2.5 mM KCl, 2.5 mM $MgSO_4$, 10 mM (+)-D-glucose). Thereafter, the cells were incubated for 20 min at 22 °C with the tested compounds. A range of concentrations of the compounds was used to generate data for calculating the concentration of inhibitor resulting in 50% of the effect (i.e, EC_{50}, or the concentration of the competitor inhibiting glycine uptake of 50%). Each concentration effect was tested in quadruplicate. Uptake was started by adding 60 nM [^{3}H]glycine (15 Ci/mmol, GE Healthcare) and 25 μM nonradioactive glycine. Nonspecific uptake was determined with 10 μM ORG24598, a potent and specific GlyT1 inhibitor.[8] Plates were incubated with gentle shaking, and the reaction was stopped by aspiration of the mixture and washing three times with ice-cold uptake buffer. After addition of scintillation liquid, the plates were shaken for 3 h and radioactivity was measured by liquid scintillation on a Perkin-Elmer TopCount scintillation plate reader. The CPM value for each quadruplicate of a concentration of competing compound was averaged (y_1). Then the percent specific binding was calculated according to the equation [(y_1 − nonspecific)/(total binding − nonspecific)] × 100. An EC_{50} value, defined as the concentration of the compound causing 50% inhibition of specific binding, was calculated by linear regression analysis of the dose−response data using an Excel based computer curve-fitting program.

hGlyT2 Uptake Inhibition Assay. The assay was performed with mammalian cells, (Flp-in-CHO), transfected with hGlyT2 cDNA, using the same conditions as described for the hGlyT1 uptake assay with slight modifications. Uptake was started by the addition of 200 nM [^{3}H]glycine (without cold glycine). Nonspecific uptake was determined with 5 μM ORG25543, a potent and specific GlyT2 inhibitor,[19] and the reaction was stopped after 30 min.

Reversal of L-687,414-Induced Hyperlocomotion in Mice. Animals and Housing Conditions. Male NMRI mice (20−30 g) supplied from Iffa Credo, Lyon, France, were housed in a vivarium at controlled temperature (20−22 °C) and under a (12 h light)/(12 h dark) cycle (lights on at 6:00 a.m.). Mice were allowed ad libitum access to food and water. The experimental procedures used in the present study received prior approval from the City of Basel Cantonal Animal Protection Committee based on adherence to federal and local regulations. Behavioral experiments were conducted between 8:00 a.m. and 2:00 p.m.

Formulation of L-687,414 and Test Substances. L-687,414 ((3*R*,4*R*)-3-amino-1-hydroxy-4-methylpyrrolidin-2-one) was used as its acetic acid salt. It was prepared following a synthetic route developed at F. Hoffmann-La Roche.[35] L-687,414 acetic acid salt was dissolved in 0.9% NaCl/0.3% Tween-80 and administered at a dose of 50 mg/kg sc in a volume of 10 mL/kg body weight. Test substances were dissolved in water/0.3% Tween-80 and administered orally in a volume of 10 mL/kg body weight.

Experiment. A computerized Digiscan 16 animal activity monitoring system (Omnitech Electronics, Columbus, OH) was used to quantify locomotor activity. Data were obtained simultaneously from eight Digiscan activity chambers placed in a soundproof room with a (12 h light)/(12 h dark) cycle. Experiments were performed during the light phase between 6:30 a.m. and 5:00 p.m. Each activity monitoring chamber consisted of a Plexiglas box (41 cm × 41 cm × 28 cm; $W \times L \times H$) with sawdust bedding on the floor surrounded by invisible horizontal and

vertical infrared sensor beams. The chambers were divided by a Plexiglas cross, providing each mouse with 20 cm × 20 cm of moving space. Two animals per box were monitored simultaneously. Chambers were connected to a Digiscan analyzer linked to a computer that constantly collected the beam status information. The activity detector operates by counting the number of times the beams change from uninterrupted to interrupted status or vice versa. Records of photocell beam interruptions for individual animals were taken every 5 min over the duration of the experimental session. Mice were first treated with compounds administered po, and 15 min later, they received an sc injection of 50 mg/kg of L-687,414. Mice were then transferred from their home cages to the recording chambers for a 15 min habituation phase, allowing them free exploration of the new environment. Horizontal activity was then recorded for a 60 min time period. Data were analyzed using a Kruskal−Wallis ANOVA followed by a Mann−Whitney *t* test. For dose−response experiments the horizontal activity value for each group of animals at a given dose of GlyT1 inhibitor (y_1) was expressed as percent of L-687,414-induced hyperlocomotion and calculated according to the equation [(y_1 − vehicle horizontal activity)/(L-687,414 horizontal activity − vehicle horizontal activity)] × 100. ID_{50} values, defined as doses of each compound producing 50% inhibition of L-687,414-induced hyperlocomotion, were calculated by linear regression analysis of the dose−response data using an Excel based computer curve-fitting program.

Microdialysis Assay in Rat. Animals and Housing Conditions. Adult male Sprague−Dawley rats weighing 220−250 g were used. Rats were housed in groups of three in Makrolon cages with sawdust bedding and were maintained under an artificial (12 h light)/(12 h dark) cycle (light onset at 6 a.m.) in a temperature and humidity controlled environment. Food and water were available ad libitum. The experimental procedure received prior approval from the City of Basel Cantonal Animal Protection Committee based on adherence to federal and local regulations on animal maintenance and testing.

Test Substance. Formulation. Compound **10a** was suspended in the vehicle shortly before the administration to the rats. The composition of the vehicle was 10% methylcellulose, 15% vitamin E TPGS, 0.18% methyl 4-hydroxybenzoate, and 0.025% propyl 4-hydroxybenzoate in demineralized water.

Surgery. At 30 min before anesthesia, the rat received 0.025 mg/kg (sc) buprenorfine. The anesthesia was begun by placing the rat in an anesthesia box with isoflurane, 3−5% (vol %). The rat was then placed in a stereotaxic device equipped with dual manipulators arms and an anesthetic mask, and the anesthesia was maintained with isoflurane, 0.8−1.3 vol % (spontaneous respiration; support gas oxygen/air, 2:1). The head was shaved and the skin was cut along the midline to expose the skull from several millimeters anterior and posterior to the bregma and lambda. A small bore hole was made in the skull to allow the stereotaxical insertion of the microdialysis probe (BAS5/4, carrying a 4 mm polyacrylonitrile dialysis membrane, cutoff of 30 KD; BAS Bioanalytical Systems Inc.) in the striatum (coordinates *A* 0.2 mm, *L* 2.9 mm, *V* 7 mm). The probe was cemented into place using binary dental cement. Once the cement was firm, the wound was closed with silk thread for suture (Silkam) and the animal was removed from the stereotaxic instrument and returned to its cage. After the surgery, rats were treated with meloxicam, 1 mg/kg sc, and allowed to recover for 3−4 days before the microdialysis experiment. The body weight of the animals was measured before the surgery and in the following days to monitor the recovery of the rat from surgery.

Microdialysis Experiment. On the day of the experiment, the inlet of the implanted dialysis probe was connected to a microperfusion pump (Carnegie Medicine) and the outlet was connected to a fraction collector. The microdialysis probe was then perfused with Ringer solution (146.5 mM NaCl, 2.7 mM KCl, 1.2 mM $CaCl_2$, 0.85 mM $MgCl_2$, 1.2 mM Na_2HPO_4, 0.27 mM NaH_2PO_4, pH 7.4) at a constant flow rate of 0.5 μL/min, and perfusates were collected in 20 min aliquots (volume of 10 μL). During the experiment, the animal was free to move in its cage and had free access to water and food. The levels of glycine and other aminoacids in the dialysate became stable after 20−60 min of perfusion. The first samples of perfusate were collected to determine the baseline (pretreatment) levels of glycine. Then the rat received either vehicle or **10a** (dose of 10 mg/kg; oral gavage of compound resuspended shortly before administration in the vehicle, 10% methylcellulose, 15% vitamin E TPGS, 0.18% methyl 4-hydroxybenzoate, propyl 4-0.025% hydroxybenzoate in demineralized water (volume of administration, 10 mL/kg), and further samples of perfusate were collected for 3 h. At the end of the experiment, rats were disconnected and returned to the animal house. Rats underwent a second microdialysis experiment 36−40 h after the first experiment. Care was taken to randomize the rats in the various experimental groups.

Analysis of Microdialysate. The levels of glycine and D/L-serine in the perfusate were assayed by a modification of the procedure of Donanzi et al.[36] and Smit et al.[37] using an HPLC apparatus equipped with an electrochemical detector. Briefly, the glycine and D/L-serine present in the perfusate were derivatized using *o*-phthaldialdehyde (OPA), purified on a reverse phase column and detected by use of an amperometric detector. The derivatization procedure and the injection of the sample were automated by use of a DIONEX ASI-100 refrigerated autosampler unit. The derivatization procedure consisted of mixing 20 μL of perfusate with 10 μL of derivatization reagent (5 mg of OPA, 0.5 mL of sodium sulfite, 0.05 M, 0.5 mL of ethanol, 9 mL of borate buffer at pH 10.4). This solution was always prepared shortly before use and incubated for 4 min at 4 °C. The OPA derivatives of glycine and D/L-serine were separated on a YMC-Pack ODS-AQ (RP-C18) S-3 μm, 120 A column (length 150 mm, diameter 4 mm). The composition of the mobile phase was 0.1 M $Na_2HPO_4 \cdot 4H_2O$, 0.13 mM $Na_2EDTA \cdot H_2O$, and 10% methanol adjusted at pH 4.8 with orthophosphoric acid. Glycine and D/L-serine were detected using an ANTEC DECADE detector equipped with a VT-03 flow cell and glassy carbon electrodes. Oxidation potential was 0.8 V.

Data Calculation. Data are expressed as picomoles of glycine or D/L-serine measured in 10 μL/perfusate (this is the volume of perfusate collected in 20 min of perfusion at 0.5 μL/min). For each rat, glycine or D/L-serine levels measured in the first five samples were averaged to provide the baseline. All glycine or D/L-serine levels measured after vehicle or drug administration in the same rat were then calculated as the percent of the mean baseline and plotted vs time. **10a** was tested in three rats, and the results are expressed as the mean ± SEM.

Supporting Information Available: Preparation details of compounds **25**−**53**, **55**, **56** and their intermediates; effect of **2** and selective GlyT2 inhibitor Org-25543 in L-687,414-induced hyperlocomotion assay; hERG inhibition assay; rat and monkey pharmacokinetic measurements; HPLC trace of compounds **10a**,**b** and **25**−**56**. This material is available free of charge via the Internet at http://pubs.acs.org.

References

(1) Conn, P. J.; Tamminga, C.; Schoepp, D. D.; Lindsley, C. Schizophrenia: moving beyond monoamine antagonists. *Mol. Interventions* **2008**, *8*, 99–107.
(2) Javitt, D. C. Glutamate and schizophrenia: phencyclidine, *N*-methyl-D-aspartate receptors, and dopamine-glutamate interactions. *Int. Rev. Neurobiol.* **2007**, *78*, 69–108.
(3) Danysz, W.; Parsons, C. G. Glycine and *N*-methyl-D-aspartate receptors: physiological significance and possible therapeutic applications. *Pharmacol. Rev.* **1998**, *50*, 597–664.
(4) (a) Sur, C.; Kinney, G. G. Glycine transporter 1 inhibitors and modulation of NMDA receptor-mediated excitatory neurotransmission. *Curr. Drug Targets* **2007**, *8*, 643–649. (b) Thomsen, C. Glycine transporter inhibitors as novel antipsychotics. *Drug Discovery Today: Ther. Strategies* **2006**, *3*, 539–545.
(5) Shim, S. S.; Hammonds, M. D.; Kee, B. S. Potentiation of the NMDA receptor in the treatment of schizophrenia: focused

on the glycine site. *Eur. Arch. Psychiatry Clin. Neurosci.* **2008**, *258*, 16–27.

(6) (a) Javitt, D. C. Glycine transport inhibitors for the treatment of schizophrenia: symptom and disease modification. *Curr. Opin. Drug Discovery Dev.* **2009**, *12*, 468–478. (b) Bridges, T. M.; Williams, R.; Lindsley, C. W. Design of potent GlyT1 inhibitors: in vitro and in vivo profiles. *Curr. Opin. Mol. Ther.* **2008**, *10*, 591–601. (c) Hashimoto, K. Glycine transporter-1 inhibitors as novel therapeutic drugs for schizophrenia. *Cent. Nerv. Syst. Agents Med. Chem.* **2007**, *7*, 177–182. (d) Harsing, L. G.; Juranyi, Z.; Gacsalyi, I.; Tapolcsanyi, P.; Czompa, A.; Matyus, P. Glycine transporter type-1 and its inhibitors. *Curr. Med. Chem.* **2006**, *13*, 1017–1044. (e) Lindsley, C. W.; Wolkenberg, S. E.; Kinney, G. G. Progress in the preparation and testing of glycine transporter type-1 (GlyT1) inhibitors. *Curr. Top. Med. Chem.* **2006**, *6*, 1883–1896.

(7) Atkinson, B. N.; Bell, S. C.; De Vivo, M.; Kowalski, L. R.; Lechner, S. M.; Ognyanov, V. I.; Tham, C.-S.; Tsai, C.; Jia, J.; Ashton, D.; Klitenick, M. A. ALX 5407: a potent, selective inhibitor of the hGlyT1 glycine transporter. *Mol. Pharmacol.* **2001**, *60*, 1414–1420.

(8) Brown, A.; Carlyle, I.; Clark, J.; Hamilton, W.; Gibson, S.; McGarry, G.; McEachen, S.; Rae, D.; Thorn, S.; Walker, G. Discovery and SAR of Org 24598, a selective glycine uptake inhibitor. *Bioorg. Med. Chem. Lett.* **2001**, *11*, 2007–2009.

(9) Smith, G.; Ruhland, T.; Mikkelsen, G.; Andersen, K.; Christoffersen, C. T.; Alifrangis, L. H.; Mork, A.; Wren, S. P.; Harris, N.; Wyman, B. M.; Brandt, G. The synthesis and SAR of 2-arylsulfanyl-phenyl piperazinyl acetic acids as GlyT-1 inhibitors. *Bioorg. Med. Chem. Lett.* **2004**, *14*, 4027–4030.

(10) Egle, I.; Delaney, W.; Wang, Z.; Shumacher, R.; Hopper, A. T.; Tehim, A.; Maddarod, S. Preparation of *N*-Propenylsarcosines as Glycine Transport-1 Inhibitors (GlyT-1) for the Treatment of Neurological and Neuropsychiatric Disorders. PCT Int. Appl. WO 2002066456, 2002.

(11) Perry, K. W.; Falcone, J. F.; Fell, M. J.; Ryder, J. W.; Yu, H.; Love, P. L.; Katner, J.; Gordon, K. D.; Wade, M. R.; Man, T.; Nomikos, G. G.; Phebus, L. A.; Cauvin, A. J.; Johnson, K. W.; Jones, C. K.; Hoffmann, B. J.; Sandusky, G. E.; Walter, M. W.; Porter, W. J.; Yang, L.; Merchant, K. M.; Shannon, H. E.; Svensson, K. A. Neurochemical and behavioral profiling of the selective GlyT1 inhibitors ALX5407 and LY2365109 indicate a preferential action in caudal *vs* cortical brain areas. *Neuropharmacology* **2008**, *55*, 743–754.

(12) Dargazanli, G.; Estenne Bouhtou, G.; Magat, P.; Marabout, B.; Medaisko, F.; Roger, P.; Sevrin, M.; Veronique, C. FR Patent Appl. FR2838739, 2003.

(13) Wolkenberg, S. E. Glycine Transporter 1 (GlyT1) Inhibitors for the Treatment of Schizophrenia. *Abstracts of Papers*, 236th National Meeting of the American Chemical Society, Philadelphia, PA, August 17−21, 2008; American Chemical Society: Washington, DC, 2008; MEDI-220.

(14) Lowe, J. A.; Hou, X.; Schmidt, C.; David, T., F.; McHardy, S.; Kalman, M.; DeNinno, S.; Sanner, M.; Ward, K.; Lebel, L.; Tunucci, D.; Valentine, J. The discovery of a structurally novel class of inhibitors of the type 1 glycine transporter. *Bioorg. Med. Chem. Lett.* **2009**, *19*, 2974–2976.

(15) (a) Pinard, E.; Ceccarelli, S. M.; Stalder, H.; Alberati, D. Discovery of *N*-(2-aryl-cyclohexyl) substituted spiropiperidines as a novel class of GlyT1 inhibitors. *Bioorg. Med. Chem. Lett.* **2006**, *16*, 349–353. (b) Ceccarelli, S. M.; Pinard, E.; Stalder, H.; Alberati, D. Discovery of N-(2-hydroxy-2-aryl-cyclohexyl) substituted spiropiperidines as GlyT1 antagonists with improved pharmacological profile. *Bioorg. Med. Chem. Lett.* **2006**, *16*, 354–357. (c) Alberati, D.; Ceccarelli, S. M.; Jolidon, S.; Krafft, E. A.; Kurt, A.; Maier, A.; Pinard, E.; Stalder, H.; Studer, D.; Thomas, A. W.; Zimmerli, D. Design and synthesis of 4-substituted-8-(2-phenyl-cyclohexyl)-2,8-diaza-spiro-[4.5]decan-1-one as a novel class of GlyT1 inhibitors: achieving selectivity against the μ opioid and nociceptin/orphanin FQ peptide (NOP) receptors. *Bioorg. Med. Chem. Lett.* **2006**, *16*, 4305–4310. (d) Alberati, D.; Hainzl, D.; Jolidon, S.; Krafft, E. A.; Kurt, A.; Maier, A.; Pinard, E.; Thomas, A. W.; Zimmerli, D. Discovery of 4-substituted-8-(2-hydroxy-2-phenyl-cyclohexyl)-2,8-diaza-spiro[4.5]decan-1-one as a novel class of highly selective GlyT1 inhibitors with improved metabolic stability. *Bioorg. Med. Chem. Lett.* **2006**, *16*, 4311–4315. (e) Alberati, D.; Hainzl, D.; Jolidon, S.; Kurt, A.; Pinard, E.; Thomas, A. W.; Zimmerli, D. 4-Substituted-8-(1-phenyl-cyclohexyl)-2,8-diaza-spiro-[4.5]decan-1-one as a novel class of highly selective GlyT1 inhibitors with superior pharmacological and pharmacokinetic parameters. *Bioorg. Med. Chem. Lett.* **2006**, *16*, 4321–4325. (f) Pinard, E.; Alberati, D.; Borroni, E.; Ceccarelli, S. M.; Fischer, H.; Hainzl, D.; Jolidon, S.; Moreau, J. L.; Stalder, H.; Thomas, A. W. Design, Synthesis and Structure−Activity Relationship of N(1)-(2-Phenyl-cylohexyl)-4-amino-piperidine Derivatives as Potent and Selective Glycine Reuptake Inhibitors. *Abstracts of Papers*, 231st National Meeting of the American Chemical Society, Atlanta, GA, March 26−30, 2006; American Chemical Society: Washington, DC, 2006; MEDI-407.

(16) Pinard, E.; Alberati, D.; Borroni, E.; Fischer, H.; Hainzl, D.; Jolidon, S.; Moreau, J. L.; Narquizian, R.; Nettekoven, M.; Norcross, R. D.; Stalder, H.; Thomas, A. W. Discovery of benzoylpiperazines as a novel class of potent and selective GlyT1 inhibitors. *Bioorg. Med. Chem. Lett.* **2008**, *18*, 5134–5139.

(17) Tricklebank, M. D.; Bristow, L. J.; Hutson, P. H.; Leeson, P. D.; Rowley, M.; Saywell, K.; Singh, L.; Tattersall, F. D.; Thorn, L.; Williams, B. J. The anticonvulsant and behavioral profile of L-687,414, a partial agonist acting at the glycine modulatory site on the *N*-methyl-D-aspartate (NMDA) receptor complex. *Br. J. Pharmacol.* **1994**, *113*, 729–736.

(18) Alberati D.; Moreau J. L.; Mory R.; Pinard E.; Wettstein J. G. Unpublished results. See Supporting Information file for the effects measured with compound **2** and with the selective GlyT2 inhibitor 4-benzyloxy-*N*-(1-dimethylaminocyclopentylmethyl)-3,5-dimethoxybenzamide (Org-25543) on the L-687,414-induced hyperlocomotion in mice.

(19) Caulfield, W. L.; Collie, I. T.; Dickins, R. S.; Epemolu, O.; McGuire, R.; Hill, D. R.; McVey, G.; Morphy, J. R.; Rankovic, Z.; Sundaram, H. The first potent and selective inhibitors of the glycine transporter type 2. *J. Med. Chem.* **2001**, *44*, 2679–2682.

(20) Jolidon, S.; Narquizian, R.; Nettekoven, M. H.; Norcross, R. D.; Pinard, E.; Stalder, H. Preparation of Alkoxybenzoylpiperazines as Inhibitors of Glycine Transporter 1 (GlyT-1). PCT Int. Appl. WO 2005014563, 2005.

(21) On November 10, 2009, F. Hoffmann-La Roche Ltd. reported positive phase II results with RG1678, a potential first-in-class treatment for the negative symptoms of schizophrenia. See Investor Update, November 10, **2009**, at www.roche.com.

(22) Clark, M. T.; Coburn, R. A.; Evans, R. T.; Genco, R. J. 5-(Alkylsulfonyl)salicylanilides as potential dental antiplaque agents. *J. Med. Chem.* **1986**, *29*, 25–29.

(23) Doswald, S.; Hanlon, S. P.; Kupfer, E. Asymmetric Reduction of 1,1,1-Trifluoroacetone by *Saccharomyces cerevisiae*. U.S. Patent Appl. US009999, 2007.

(24) Yamanaka, H.; Takekawa, T.; Morita, K.; Ishihara, T. Preparation of novel β-trifluoromethyl vinamidinium salt and its synthetic application to trifluoromethylated heterocycles. *Tetrahedron Lett.* **1996**, *37*, 1829–1832.

(25) Mangalagiu, I.; Benneche, T.; Undheim, K. Trialkylalanes in palladium-catalyzed chemo- and regioselective alkylations. *Tetrahedron Lett.* **1996**, *37*, 1309–1312.

(26) Lipophilicity was calculated with the clogP, version 4.94, program (BioByte Corp., Claremont, CA, http://www.biobyte.com).

(27) Gerber Molecular Design, Amden, Switzerland, http://www.moloc.ch.

(28) Fischer, H.; Kansy, M. Automated Generation of Multi-Dimensional Structure Activity and Structure Property Relationships. PCT Int. Appl. US 2007027632, 2007.

(29) Jamieson, C.; Moir, E. M.; Rankovic, Z.; Wishart, G. Medicinal chemistry of hERG optimizations: highlights and hang-ups. *J. Med. Chem.* **2006**, *49*, 5029–5046.

(30) For a recent review on the molecular basis of hERG channel interaction, see the following: Thai, K. M.; Ecker, G. F. Predictive models for hERG channel blockers: ligand-based and structure-based approaches. *Curr. Med. Chem.* **2007**, *14*, 3003–3026.

(31) Shengguo, S; Adejare, A. Fluorinated molecules as drugs and imaging agents in the CNS. *Curr. Top. Med. Chem.* **2006**, *14*, 1457–1564.

(32) Boehm, H.-J.; Banner, D.; Bendels, S.; Kansy, M.; Kuhn, B.; Mueller, K.; Obst-Sander, U.; Stahl, M. Fluorine in medicinal chemistry. *ChemBioChem* **2004**, *5*, 637–643.

(33) The panel consisted of targets included in the standard CEREP high throughput profile screen complemented with enzymes (phosphodiesterases, kinases, MAO-A, COMT, acetylcholineesterase): http://www.cerep.fr.

(34) Kansy, M.; Senner, F.; Gubernator, K. Physicochemical high throughput screening: parallel artificial membrane permeation assay in the description of passive absorption processes. *J. Med. Chem.* **1998**, *41*, 1007–1010.

(35) Pinard, E.; Burner, S.; Cueni, P.; Montavon, F.; Zimmerli, D. A short and efficient synthesis of the NMDA glycine site antagonist: (3*R*,4*R*)-3-amino-1-hydroxy-4-methyl pyrrolidin-2-one (L-687,414). *Tetrahedron Lett.* **2008**, *49*, 6079–6080.

(36) Donzanti, B. A.; Yamamoto, B. K. An improved and rapid method for the isocratic separation of aminoacid neurotransmitters from brain tissue and microdialysis perfusate. *Life Sci.* **1988**, *43*, 913–922.

(37) Smit, S.; Sharp, T. Measurement of GABA in rat brain microdialysate using *o*-phthalaldialdehyde-sulphite derivatization and high performance liquid chromatography with electrochemical detection. *J. Chromatogr.* **1994**, *652*, 228–233.